Quantitative Determination of Phase Content in Multiphase Polymers by Combining Spin-Diffusion and CP-MAS NMR

L. Zhang,[†] Z. Liu,[†] Q. Chen,*[,†] and E. W. Hansen*[,‡]

Physics Department and the State Key Laboratory of Precision Spectroscopy, East China Normal University, 3663 Northern Zhongshan Road, Shanghai 200062, People's Republic of China, and Department of Chemistry, University of Oslo, P.O. Box 1033 Blindern, N-0315 Oslo, Norway

Received April 2, 2007; Revised Manuscript Received June 2, 2007

ABSTRACT: We present a new approach to determine quantitatively the phase content of multiphase polymers by applying a spin-diffusion pulse sequence (filter) prior to cross-polarization (CP) in a ^{13}C-CPAS experiment. The technique is exemplified for two rather different polymer systems, a high-density polyethylene (HDPE) and four styrene−isoprene diblock copolymers, all of known phase contents. In principle, the technique should be applicable to any multiphase system in which spin-diffusion between different regions/phases exists and where the magnetization of phases can selectively be filtered out.

Introduction

Cross-polarization (CP) from abundant spins (*I*) to dilute spins (*S*) combined with magic-angle spinning (MAS) and high-power decoupling have been shown to be the most important technique to obtain a solid-state high-resolution NMR spectrum of nucleus *S* with an optimum signal-to-noise ratio.[1,2] The technique has been widely applied to probe the molecular structure of organic and inorganic solids since its discovery by Pines et al. in 1973.[2] CP overcomes two common problems in the NMR of solids. The first stems from the low inherent sensitivity of dilute nuclei, such as ^{13}C, ^{29}Si, and ^{15}N (isotopic abundance of 1.1%, 4.7%, and 0.03%, respectively). The second difficulty relates to the potentially and inherently long relaxation times (tens of seconds for ^{13}C in powdered organics and minutes for ^{29}Si in framework silicates) frequently found for dilute spin-$^1/_2$ nuclei, possessing low gyromagnetic ratio. As a consequence, this necessitates a long time delay between consecutive scans. When several thousand scans are required to obtain a reasonable signal-to-noise ratio, the sampling time may become unreasonably long. This problem may be overcome by CP, i.e., by transfer of magnetization from abundant spins (possessing a short relaxation time) to dilute spins (possessing a long relaxation time).

However, the significant gain in sensitivity obtained by applying the CP technique has a certain price; i.e., the resulting spectrum may not be quantitative. This is because the final signal intensity observed in a CP spectrum is controlled by several competitive relaxation processes, as for instance the transfer of magnetization between *I*-spins and *S*-spins (described by a characteristic time T_{IS}), the transfer of magnetization between the *I*-spins and the lattice within the rotating frame of reference (described by a relaxation time $T^{\mathrm{I}}_{1\rho}$), and the transfer of magnetization between *S*-spins and the lattice in the rotating frame (described by a relaxation time $T^{\mathrm{S}}_{1\rho}$). However, frequently $T^{\mathrm{S}}_{1\rho}$ is found to be significantly longer than T_{IS}, so the former relaxation process is of minor importance within the CP dynamics.

Of particular importance, similar ^{13}C-spins confined in various phases in a polymer sample reveal generally different degree of polarization at the same contact time in a CP experiment. For instance, within the same polymer the two time parameters $T^{\mathrm{H}}_{1\rho}$ and T_{CH} may be different for a crystalline phase and an amorphous phase, respectively, due to different molecular mobility. This makes a quantitative estimate of crystallinity uncertain. This is rather unfortunate, since information regarding phase distribution and degree of cross-linking, etc. are of major significance and concern in polymer chemistry.

The simplest way to obtain a quantitative ^{13}C spectrum is to accumulate single Bloch decays with a recycle delay longer than 5 times the longest ^{13}C T_1. However, as already mentioned, this is not generally appropriate because the overall sampling time might become intolerably long. Several and different approaches have been proposed to render CP experiments quantitative. A common technique is to perform a series of CP measurements by varying the contact time.[3] Zhang et al.[4] reported a so-called polarizing−depolarizing scheme (PDS) in which a depolarization period was introduced into a conventional CP pulse sequence. By acquiring three intensity distorted spectra, they were able to derive quantitatively comparable signals of the individual rare spin signals.

Fu et al.[5] presented recently a Lee−Goldburg (LG) frequency modulated CP scheme and demonstrated that the LG sequence significantly lengthened the $T^{\mathrm{H}}_{1\rho}$ and the frequency modulation shortened the cross-polarization time for nonprotonated *S*-spins. A combination of these two experiments was claimed to improve quantification of the spectrum. Although this experimental setup reduces the overall sampling time compared to a direct-polarization (DP) ^{13}C NMR experiment, the introduction of spectral manipulation and calculations renders the method somewhat less straightforward.

Also, Hu and co-workers[6] combined the spectral information obtained from four different ^{13}C experiments (among which two of the experiments were CP-based) to determine the crystallinity of an ultradrawn ultrahigh molecular weight PE. Their result was in agreement with the corresponding value determined by ^{1}H NMR and from sample density. Also, Deng and co-workers published recently an experimental scheme for achieving uniform CP enhancement of low-γ nuclear species in solids under MAS conditions, termed quantitative cross-polarization, or QUCP. However, their method was not aimed at quantifying phase content of multiphase polymers.[7]

* Corresponding authors. E-mail: qchen@ecnu.edu.cn or eddywh@kjemi.uio.no.
[†] East China Normal University.
[‡] University of Oslo.

10.1021/ma0707786 CCC: $37.00
Published on Web 06/30/2007

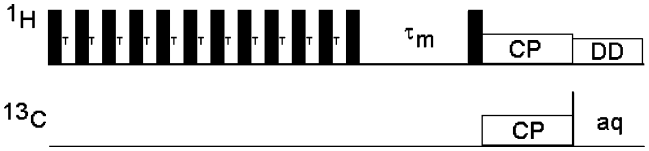

Figure 1. Schematic view of the pulse sequence applied in this work. See Experimental Section for more details.

The key factor needed in order to obtain quantitative information from a CPMAS experiment relies on the so-called enhancement factor η, which varies with the CP contact time. Theoretically, for a carbon nucleus with nearby protons the maximum $\eta = \gamma_H/\gamma_C \sim 4$. In real practice, it is difficult to reach this theoretical value due to existence of various relaxation mechanisms, like ^{1}H and ^{13}C spin−lattice relaxation in rotating frame. Because of variation in the chemical and physical environment of a carbon nucleus, the strength of the C−H dipolar interaction, and the molecular motion, the η factor may vary significantly from one carbon to another. It is not possible in practice to have a contact time that allows different carbons to be polarized to the same degree simultaneously. This is the key factor, which makes the CP spectra nonquantitative. VanderHart and Khoury[8] reported on some high-density polyethylene (HDPE) measurements using CP with a contact time between 0.7 and 2 ms and found η to be 3.5 ± 0.2 for carbons confined within the crystalline region and 2.4−3.0 for carbons confined within the amorphous region, respectively.

In this work, we will show how the phase content within a polymer can be determined quantitatively by combining spin-diffusion (SD) and CP-MAS. Actually, the technique gives the enhancement factor of the different phases, on a relative scale. The application of the technique is exemplified using two different types of polymers: a high-density polyethylene (HDPE) and styrene−isoprene diblock copolymers (PS−PI) with known phase contents.

Experimental Section

Materials. The polymer material chosen for testing the quantitative SD/^{13}C-CPMAS technique was a high-density polyethylene (HDPE) received from Showa Denko (Sholex-6050; $M_w = 4.6 \times 10^4$ g/mol) which was melted at 130 °C and subsequently quenched in liquid nitrogen, obtaining a crystallinity of $59 \pm 2\%$.[9] The four polystyrene (PS)−polyisoprene (PI) diblock copolymers were obtained "in-house" with well-defined phase contents of PS of 72% (S1), 58% (S2), 54% (S3), and 68% (S4). Their molecular weights M_n were 3.0×10^4 g/mol (S1), 1.9×10^4 g/mol (S2), 2.43×10^4 g/mol (S3), and 3.9×10^4 g/mol, respectively. All samples possessed narrow weight distributions with $M_w/M_n < 1.07$. The powder PS−PI samples were studied as received without further treatment.

NMR Measurement. High-resolution solid-state ^{13}C NMR measurements were carried out at room temperature (22 °C) on a Bruker DSX-300 spectrometer operating at 75.47 MHz. The PE sample was crushed and packed into a magic angle spinning (MAS) rotor, having a diameter of 4 mm. The MAS rate was set to 5 kHz, and the ^{1}H pulse width was set to 2.6 μs. ^{13}C chemical shifts were referenced to the chemical shift of the carbonyl carbon signal (176.03 ppm) of glycine. The contact time within the conventional CP part of the pulse sequence was varied between 0.5 and 10 ms. The strength of the B_1 field was 55.5 kHz (carbon channel) and 56.8 kHz (proton channel). A TPPM decoupling pulse sequence was applied for proton decoupling. The actual pulse sequence is illustrated in Figure 1 with a time delay τ of 8 μs between pulses in the "filter part" of the sequence, causing a depletion of the rigid phase signal due to its much stronger dipolar−dipolar coupling. A total of 160 scans were accumulated with a repetition time of 5 s between the scans. The diffusion time (τ_m) was set to less than 30 ms in order to avoid proton T_1 effects/corrections. As for the reliability and stability, control experiments under different Hartmann−Hahn conditions using a contact time of 2 ms were carried out as well.

Theory

In a conventional CP experiment the enhancement factor η of dilute spins S via polarization transfer from abundant spins I is defined as

$$\eta = \frac{M^{CP}(S)}{M^0(S)} \tag{1}$$

where $M^0(S)$ is the equilibrium magnetization, or Boltzmann magnetization, and $M^{CP}(S)$ represents the CP-enhanced magnetization of the S-spins.[2,8] From basic NMR theory,[3,5,10−12] the enhancement factor η can be written

$$\eta = \eta(\tau_{cp}; T^I_{1\rho}, T_{SI})$$
$$= \eta_{ideal} \frac{1}{1 - T_{SI}/T^I_{1\rho}} [\exp(-\tau_{cp}/T^I_{1\rho}) - \exp(-\tau_{cp}/T_{SI})] \tag{2}$$

where τ_{cp} is the contact time between the I-spins and the S-spins during cross-polarization and $T^I_{1\rho}$ and T_{IS} define the rotating frame spin−lattice relaxation time of the I-spins and the cross-polarization time between the S- and I-spins, respectively. Equation 2 is derived from classical CP theory and is strictly valid for a dilute-abundant spin system (i.e., a C/H system) for $T_{IS}/T^S_{1\rho} \ll 1$. It is generally not possible to find a contact time that allows carbons in different chemical or physical environments to be simultaneously polarized to the same degree (cf. eq 2). Moreover, it is implicitly assumed that the contact time τ_{cp} is large enough to avoid oscillatory kinetic behavior due to spin-diffusion. If not ($\tau_{cp} \leq 1$ ms),[3] eq 2 should be replaced by an oscillatory type of function which is discussed thoroughly elsewhere.[3]

We will take PE as a model system to illustrate our strategy. By assuming that PE consists only of a crystalline (C) and an amorphous (A) phase with $M^{CP}_C(S)$ and $M^{CP}_A(S)$ representing the CP enhanced ^{13}C magnetizations within the two phases, and $M^0_C(S)$ and $M^0_A(S)$ denoting the respective ^{13}C Boltzmann magnetizations, it follows that the quantitative ratio (ϕ) between the Boltzmann magnetizations of the two phases can be written

$$\phi = \frac{M^0_C(S)}{M^0_A(S)} = \frac{\eta_A}{\eta_C} \frac{M^{CP}_C(S)}{M^{CP}_A(S)} \tag{3}$$

where η_C and η_A define the enhancement factors at a certain contact time of the crystalline (C) and the amorphous (A) phases, respectively. It is evident that quantitative analysis can be made if the ratio of enhancement factors is known. Moreover, under the same experimental conditions it is known that $M^{CP}(S)$ is proportional to the proton magnetization ($M(I)$), i.e. $M^{CP}(S) = KM(I)$, where K is a constant. This relation is actually the basis of measuring ^{1}H relaxation times via ^{13}C CP/MAS. Because the proton magnetizations of the different phases are quantitatively comparable, it follows that the ratio ϕ (cf. eq 3) can be derived from the respective proton magnetizations:

$$M^{CP}_C(S) = K_C M_C(I); \quad M^{CP}_A(S) = K_A M_A(I) \tag{4}$$

where $M_C(I)$ and $M_A(I)$ denote the proton magnetizations of the crystalline phase and the amorphous phase, respectively, hence

$$\phi = \frac{M_C(I)}{M_A(I)} = \frac{K_A}{K_C}\frac{M_C^{CP}(S)}{M_A^{CP}(S)} \quad (5)$$

When comparing eq 3 and eq 5, we obtain the important result

$$\frac{\eta_A}{\eta_C} = \frac{K_A}{K_C} \quad (6)$$

showing that the ratio of enhancement factors η_A/η_C is equivalent to the ratio K_A/K_C. Figure 1 shows the pulse sequence employed in the present work. During the spin-diffusion part of the pulse sequence, the proton magnetization of the crystalline phase is filtered out by a proper choice of the interpulse time τ, leaving the proton magnetization of the amorphous phase unchanged and amenable for further manipulation. In principle, we do not need to have a "clear" initial condition; in other words, it is not necessary to filter out the magnetization of the crystalline phase completely. The purpose of applying a dipolar-filter sequence is just to create a gradient of magnetization between the different phases. During the diffusion period τ_m, the proton magnetization will redistribute between the phases. If choosing a spin diffusion time τ_m (cf. Figure 1) different from 0, the proton magnetization will diffuse into the crystalline phase during the time interval τ_m. If we denote by $M_A(I;0)$ the total initial proton magnetization, and keeping in mind that $M_A(I;0)$ is conserved during the experiment (if no proton lab-frame spin−lattice relaxation takes place), it follows that

$$M_A(I;0) = M_C(I;\tau_m) + M_A(I;\tau_m) \quad (7)$$

where $M_C(I;\tau_m)$ and $M_A(I;\tau_m)$ define the proton magnetizations within the crystalline and the amorphous phases after time τ_m, respectively. By inserting eq 4 into eq 7, we derive the following important equation:

$$M_A(I;0) = M_C^{CP}(S;\tau_m)/K_C + M_A^{CP}(S;\tau_m)/K_A \quad (8)$$

which by multiplying by K_C on both sides reads

$$M_C^{CP}(S;\tau_m) = -\frac{K_C}{K_A}M_A^{CP}(S;\tau_m) + K_C M_A(I;0) \quad (9a)$$

Because $M_C^{CP}(S;\tau_m)$ and $M_A^{CP}(S;\tau_m)$ are obtained experimentally and $M_A(I;0)$ is constant and independent of τ_m, it follows that K_A/K_C and consequently η_A/η_C (cf. eq 6) can be determined from a minimum of two CP-based spectra acquired at different τ_m. The relative phase content can then be determined by performing an additional and conventional CP-MAS experiment, acquired under the same experimental conditions (same contact time). Compared to previous reports, this method is apparently time-saving. Furthermore, by implementing eq 4 into eq 9a and dividing by $M_A^{CP}(S;0)$on both sides of the equations, we obtain a normalized equation:

$$\frac{M_C^{CP}(S;\tau_m)}{M_A^{CP}(S;0)} = -\frac{K_C}{K_A}\frac{M_A^{CP}(S;\tau_m)}{M_A^{CP}(S;0)} + \frac{K_C}{K_A} \quad (9b)$$

implying that the K_C/K_A ratio is represented by the slope of the straight line, defined by the normalized C-magnetization against the A-magnetization of the *S*-spins, respectively. The normalization constant in eq 9b, $M_A^{CP}(S;0)$, can easily be found by extrapolating $M_A^{CP}(S;0)$ against $\tau_m^{1/2}$. Actually, this curve is linear for short τ_m.

In the case that the filter does not operate ideally due to pulse imperfections or that the timing between successive $\pi/2$-pulses (τ) is not correctly set, some *I*-spin magnetization $M_C^0(I)$ may appear in the crystalline region C at time $\tau_m = 0$. However, the sum of magnetizations from both phases will still be conserved, resulting in a slightly modified expression for the *S*-spin magnetization as a function of τ_m

$$M_C^{CP}(S;\tau_m) = -\frac{K_C}{K_A}M_A^{CP}(S;\tau_m) + M_C^{CP}(S;0) + \frac{K_C}{K_A}M_A^{CP}(S;0) \quad (10a)$$

which, after normalization (dividing both sides of eq 10a by $M_A^{CP}(S;0)$), reads

$$\frac{M_C^{CP}(S;\tau_m)}{M_A^{CP}(S;0)} = -\frac{K_C}{K_A}\frac{M_A^{CP}(S;\tau_m)}{M_A^{CP}(S;0)} + \frac{M_C^{CP}(S;0)}{M_A^{CP}(S;0)} + \frac{K_C}{K_A} \quad (10b)$$

Equation 10b shows that the slope K_C/K_A of the straight line $M_C^{CP}(S;\tau_m)/M_A^{CP}(S;0)$ vs $M_A^{CP}(S;\tau_m)/M_A^{CP}(S;0)$ remains the same independent of the quality of the filter. However, the intercept of the line with the $M_A^{CP}(S;\tau_m)/M_A^{CP}(S;0)$ axis will be shifted by $M_C^{CP}(S;0)/M_A^{CP}(S;0)$ relative to the corresponding intercept obtained for an ideal filter (cf. eq 9b). In conclusion, the same K_C/K_A ratio will be obtained, independent of the filter quality.

Although the above method is exemplified by a two-phase system, it can easily be generalized to a multiphase system, provided that each phase possesses at least one resolvable signal in the CP-MAS spectrum, and a magnetization gradient across the different phases can be created from the dipolar filter. Supposing that *n* phases exist in a sample, the following equation can easily be derived, according to the above procedure

$$\sum_1^n \frac{M_i^{CP}(S;\tau_m)}{K_i} = \frac{M_n^{CP}(S;0)}{K_n} \quad (11a)$$

where the signals from all phases, except for the nth phase, are filtered out (ideal filter). For a nonideal filter, eq 11a can be generalized to read

$$\sum_1^n \frac{M_i^{CP}(S;\tau_m) - M_i^{CP}(S;0)}{K_i} = 0 \quad (11b)$$

where $M_i^{CP}(S,\tau_m)$ is the CP enhanced signal intensity of the characteristic peak of the ith phase. K_i is a constant for each phase I (cf. eq 4), and $\sum_i^n M_i^{CP}(S;0)$ represents the initial *S*-magnetization, after filtration. Hence, by measuring a minimum of *n* spectra at different τ_m, eq 11b gives rise to a set of *n* linear equations (one equation for each τ_m) which can be solved for the K_i/K_j ratios, by solving the resulting set of linear equations. In the discussion that follows we will use the short hand notation $K_{X/Y}$ to mean the ratio between K_X and K_Y, i.e.; $K_{X/Y} = K_X/K_Y$. Also, the symbols S and CP will be excluded from all subsequent equations in order to present the equations in a more readable form where ambiguity is not causing a problem.

Notably, the proposed method is not limited to C/H systems only but is of more general applicability.

Results and Discussion

HDPE. A ^{1}H NMR FID of the HDPE sample is shown in Figure 2, from which the crystallinity was calculated by model

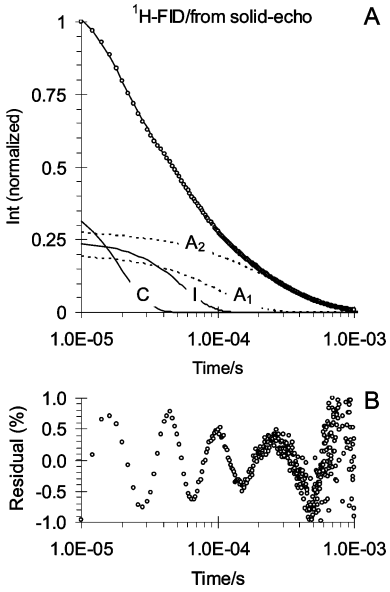

Figure 2. (A) ^{1}H NMR FID taken from the solid echo of the high-density PE sample. The position of the echo was located at time 10 μs after the application of an rf pulse of ca. 2 μs. The open dots (○) are experimental points and were sampled every 2 μs. The solid curve represents model fit according to a procedure which is detailed in ref 14. The four distinctive components C, I, A_1, and A_2 define the crystalline, the intermediate, and the noncrystalline components, respectively. (B) Difference between observed and model-fitted data.

fitting according to a procedure outlined by Hansen and co-workers.[14] The solid curve going through the observed data points represents such a nonlinear least-squares model fit to the observed data and is discussed in detail elsewhere.[13−15] We simply state that a total of four separate functions were needed to fit the observed FID. The two significantly shorter T_2 components (denoted C and I in Figure 2; solid curves) were assigned the crystalline and the intermediate components, respectively, and contributed 59 ± 2% to the overall signal intensity and was ascribed the crystalline fraction of the sample.[14] Although the residual (Figure 2B) is rather small, its oscillating behavior signifies some systematic error. However, this effect is of minor concern regarding the estimation of crystallinity.[14] It should be noted that the phase composition, as characterized by the present technique, is affected to some extent by the temperature of the experiment and the fitting function used for the deconvolution of the FID into the separate components.[15,16] Litvinov et al.[15] suggested that a proper temperature for the NMR experiment should exceed the dynamic glass transition temperature, i.e., an optimum temperature around 100 °C. However, the temperature should not be too high to prevent annealing of the sample during the NMR experiment. Also, the solid-echo experiment may lead to a systematic underestimation of the phase composition with increasing pulse spacing (t_{se}) in the solid-echo experiment due to (i) an incomplete refocusing of the dipolar interactions, (ii) molecular motions defined by a correlation time of which is comparable to the pulse spacing, and (iii) the shift of the echo maximum caused by a nonzero pulse width. In the above analysis we have corrected for these effects by adjustment of the amplitude of the respective phases derived from a solid-echo experiment by their respective T_2s. As is well-known,[13,14,17] the crystallinity obtained by the above procedure is much more reliable than the corresponding crystallinity obtained from the ^{1}H NMR FT spectrum, due to the effects of dead time and finite pulse lengths.[14]

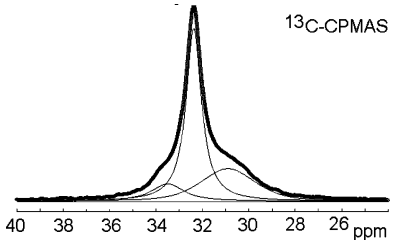

Figure 3. ^{13}C-CPMAS NMR spectrum of the PE sample obtained by applying the pulse sequence in Figure 1 by excluding the SD part of the pulse sequence and choosing τ_{cp} = 1 ms. The spectrum reveals three resonance peaks: C_1 (δ_{C_1} = 33.0 ppm), C_2 (δ_{C_2} = 32.4 ppm), and A (δ_A = 30.7 ppm). The solid curves represent nonlinear least-squares fit to three pseudo-Voigt functions (linear combination of a Lorentzian and a Gaussian function).

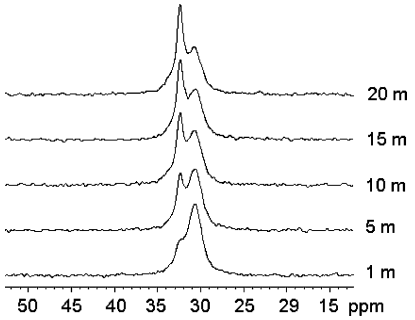

Figure 4. Series of ^{13}C-CPMAS NMR spectra with a fixed contact time τ_{cp} = 1 ms and various diffusion times τ_m (= 1, 5, 10, 15, and 20 ms; bottom to top) as obtained by applying the pulse sequence shown in Figure 1.

Moreover, because of the significantly better spectral resolution obtainable by ^{13}C NMR (Figure 3), this technique is potentially better than ^{1}H NMR when aiming at probing the relative phase content, especially in the case of multiphase systems. The spectrum presented in Figure 3 is a ^{13}C CP-MAS spectrum of the HDPE sample acquired with a contact time τ_{cp} = 1 ms. The resonance line at 32.4 ppm is assigned to the crystalline component of orthorhombic structure, whereas the broader up field peak, centered at 30.7 ppm, is ascribed to the noncrystalline, amorphous phase.[18−20] In addition, the small downfield peak at 33.7 ppm is assigned to another crystalline component possessing a monoclinic structure.[18,21]

The most important issue of our method is to obtain the $K_{C/A}$ ratio (eq 6) between phases C and A. Applying the pulse sequence illustrated in Figure 1, a gradient of ^{1}H magnetization is initially created by the "selection" portion of the pulse sequence, which consists of 12 $\pi/2$ pulses (8 μs interpulse delay). A stacked plot of some spin-diffusion ^{13}C spectra with a contact time τ_{cp} = 10 ms acquired at various diffusion times τ_m (= 1, 5, 10, 15, and 20 ms; bottom to top) are illustrated in Figure 4. The intensities of both the A- and C-magnetizations $M_A(\tau_m)$ and $M_C(\tau_m)$ are plotted as a function of the square-root of diffusion time ($\tau_m^{1/2}$) in Figure 5A, from which the normalization constant $M_A(0)$ is determined (= (7.43 ± 0.01) × 10^{10}) and enables a plot of $M_C(\tau_m)/M_A(0)$ as a function of $M_A(\tau_m)/M_A(0)$ to be constructed (Figure 5B). From this latter plot we obtain $K_{C/A}$ = 1.56 ± 0.14, and $M_C(0)/M_A(0) + K_{C/A}$ = 2.26 ± 0.01 (cf. eq 5b). By combining these two latter parameters, we obtain $M_C(0)/(M_C(0) + K_{C/A}M_A(0)) = 0.31 \pm 0.03$, which reflects the fraction of C-magnetization remaining after the "filter" has been applied. That the filter does not operate optimal can be visually realized by referring to the last spectrum in Figure 4, which reveals a significant low-field shoulder, even at a diffusion time of τ_m = 1 ms.

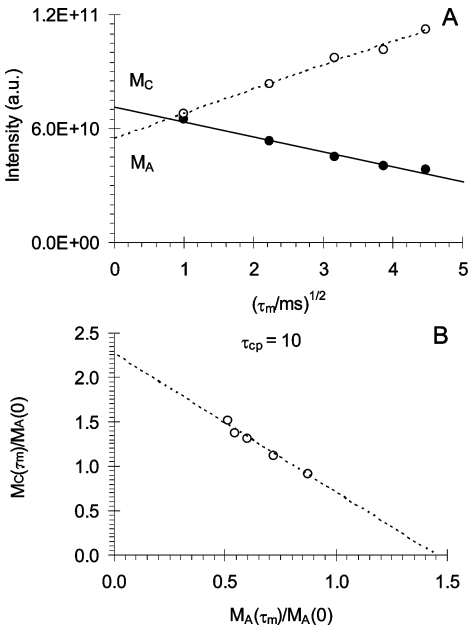

Figure 5. (A) Crystalline ($M_C(\tau_m)$) and amorphous ($M_A(\tau_m)$) signal intensities as a function of the square-root of diffusion time ($\tau_m^{1/2}$) with $\tau_{cp} = 10$ ms and $\tau_m = 1$, 5, 10, 15, and 20 ms. The straight lines represent best fit curves within the linear regions. (B) Normalized crystalline phase intensity $M_C(\tau_m)/M_A(0)$ as a function of the amorphous phase normalized signal intensity $M_A(\tau_m)/M_A(0)$ based on the data in (A). The dotted curve represents a linear best fit curve to eq 10b with $K_{C/A} = \eta_C/\eta_A = 1.56 \pm 0.14$ and $M_C(0)/M_A(0) + K_{C/A} = 2.26 \pm 0.10$.

By performing a simple ^{13}C-CPMAS experiment, an apparent crystallinity fraction f_C^{app} may be determined from the observed A- and C-magnetizations (M_A and M_C) by applying eq 12a:

$$f_C^{app} = \frac{M_C}{M_C + M_A} \tag{12a}$$

The actual "two-phase" crystallinity $f_C^{(2)}$ is then easily derived

$$f_C^{(2)} = \frac{M_C}{M_C + K_{C/A}M_A} = \frac{1}{1 + (1/f_C^{app} - 1)K_{C/A}} \tag{12b}$$

and enables the crystallinity to be determined quantitatively from ^{13}C-CPMAS if the $K_{C/A}$ ratio is known (cf. eq 6) The latter parameter is determined by SD experiments (eq 10b). From the present experiments this results in a crystallinity $f_C^{(2)} = 61 \pm 3\%$ (Table 1).

Before proceeding further, we introduce the "filter factor" ϵ, defined by

$$1 - \epsilon = \frac{M_C(0)}{M_C(0) + K_{C/A}M_A(0)} \tag{13a}$$

If performing SD experiments on the same sample and keeping all instrumental parameters unchanged and just varying the cross-polarization time τ_{cp} in the experiment, this parameter (ϵ) is expected to be constant. As can be inferred from eq 8a, ϵ attains the value 1 if the pulse sequence in Figure 1 enables to filter out all C-magnetization; otherwise, $0 < \epsilon \leq 1$. It follows from eq 10b that the intercepts (x_0 and y_0) of this straight line with the $M_A(\tau_m)/M_A(0)$ axis and the $M_C(\tau_m)/M_A(0)$ axis, respectively, can be expressed by

$$x_0 = \frac{1}{\epsilon}$$

$$y_0 = \frac{1}{\epsilon}K_{C/A} \tag{13b}$$

Figure 6 shows $M_C(\tau_m)/M_A(0)$ as a function of $M_A(\tau_m)/M_A(0)$ for different contact times τ_{cp}. In particular, we note that within experimental error all curves intercept with the $M_A(\tau_m)/M_A(0)$ axis at the same point $x_0 = 1.43 \pm 0.03$, as expected from eq 13b. Furthermore, the intercept (y_0) of the line with the $M_C(\tau_m)/M_A(0)$ axis is seen to increase with increasing contact time and is in accordance with eq 13b, since also $K_{C/A}$ (defined by the slope of the line in eq 10b) is seen to increase with contact time. Moreover, the filter efficiency in all measurements was found to be independent of the contact time τ_{cp} and equal to $\epsilon = 71 \pm 4\%$. All numerical values from the present analysis are summarized in Table 1 and show an excellent internal consistency (cf. eq 10b).

It is noted that for short contact times ($\tau_{cp} \leq 1$ ms) $K_{C/A}$ decreases with increasing τ_{cp} (Table 1), which can be rationalized by referring to eq 2 by inserting a proper choice of relaxation time parameters (not shown).

We measured the proton spin−lattice relaxation time to be ~1.2 s. Because of spin-diffusion, it was not been possible to separate the proton relaxation times for the two respective phases. However, recalling that all experiments were performed with a diffusion time τ_D of less than 25 ms there is no reason to believe that the present results are affected by spin−lattice relaxation time effects. At least, no experimental sign of any spin−lattice relaxation effects was noted in the present measurements.

The average crystallinity calculated from all the data in Table 1 amounts to $\bar{f}_C^{(2)} = 60 \pm 3\%$. This error is identical to the error estimate in each individual measurement (for each τ_{cp}) and shows that the crystallinity obtained by the present method is independent of the actual contact time used in the CP part of the pulse sequence, except for the smaller τ_{cp} of 0.5 and 1 ms, respectively. In this latter case, a slightly smaller estimated crystallinity of $f_C^{(2)} = 55.0 \pm 1.5\%$ was obtained. The reason for this is believed to originate from spatial inhomogeneity, since the crystalline region contains a small amount of a monoclinic structure that coexists with the much larger fraction of an orthorhombic structure. Since no signal oscillation was observed during the spin diffusion interval applied in this work, we have no reason to believe that any transient oscillations during CP at shorter diffusion times will affect the final estimate of the crystallinity.

Concerning the reliability and stability of the experimental technique, control experiments on a HDPE sample (quenched in liquid nitrogen followed by hammering and possessing about 50% crystallinity) performed under different Hartmann−Hahn conditions using a fixed contact time of 2 ms were carried out.

Table 2 suggests that neither $K_{C/A}$ nor the corresponding crystallinity fraction (as derived by the method just outlined) is affected by changing the strength of the rf power (and thus the time duration of the $\pi/2$ rf pulse) by more than 35%. Within experimental error, our proposed model therefore seems to be stable and reliable under different Hartmann−Hahn conditions.

However, one aspect of concern relates to the implicit approximation of treating an actual "three-phase" system as a "two-phase" system. The former is clearly evidenced by the two observed peaks (I and C) within the crystalline region of the ^{13}C-CPMAS spectrum (cf. Figure 3). When performing a "three-peak" fit to the spectra for each diffusion time τ_m, it was

Table 1. $K_{C/A}$ Ratio, Apparent Crystallinity Fraction f_C^{app}, Derived Two-Phase Crystallinity Fraction $f_C^{(2)}$, Intercept y_0, and Filter Efficiency ϵ as a Function of Contact Time τ_{cp}, As Derived by a Combined ^{13}C-SD/CPMAS Pulse Sequence (Figure 1)

t_{cp} (ms)	$K_{C/A} = \eta_C/\eta_A$ (eq 10b)[a]	f_C^{app}/% (eq 12a)[b]	$f_C^{(2)}$/% (eq 12b)	y_0[c]	ϵ (eq 13a)
0.5	1.21 ± 0.05	61	56 ± 2	1.54 ± 0.04	0.79 ± 0.01
1	1.24 ± 0.07	59	54 ± 3	1.72 ± 0.04	0.72 ± 0.02
2	0.94 ± 0.05	59	60 ± 3	1.37 ± 0.06	0.68 ± 0.03
3	0.97 ± 0.05	61	62 ± 2	1.29 ± 0.03	0.75 ± 0.01
4	1.02 ± 0.06	62	62 ± 2	1.48 ± 0.04	0.69 ± 0.02
5	0.98 ±0.06	63	63 ± 2	1.37 ± 0.04	0.72 ± 0.02
6	1.21 ± 0.16	64	60 ± 5	1.74 ± 0.05	0.70 ± 0.04
7	1.26 ± 0.06	66	61 ± 2	1.80 ± 0.11	0.70 ± 0.02
8	1.36 ± 0.09	68	61 ± 3	1.97 ± 0.06	0.69 ± 0.02
9	1.34 ± 0.12	69	62 ± 3	2.08 ± 0.09	0.64 ± 0.04
10	1.56 ± 0.14	71	61 ± 3	2.26 ± 0.10	0.69 ± 0.03

[a] Defined by the slope of eq 10b (cf. Figure 6). [b] Determined from CPMAS only (no spin-diffusion). [c] Defined by the intercept of eq 10b with the $M_C(\tau_m)/M_A(0)$ axis (cf. Figure 6).

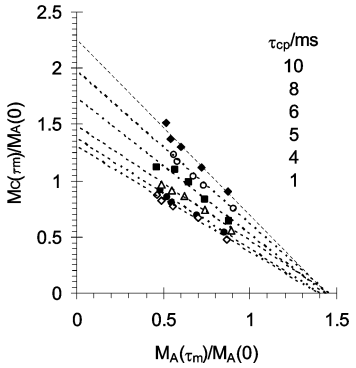

Figure 6. Normalized crystalline phase signal intensity $M_C(\tau_m)/M_A(0)$ as a function of the normalized amorphous phase signal intensity $M_A(\tau_m)/M_A(0)$ as a function of different contact times $\tau_{cp} = 10$, 8, 6, 5, 4, and 1 ms. The plotted data are based on the same type of analysis as shown in Figure 5.

Table 2. $K_{C/A}$ Ratio (Eq 6) and Corresponding Derived Crystallinity Fraction $f_C^{(2)}$ (Eq 12b) as a Function of the Strength of the RF Power (or the Time Duration of the $\pi/2$ RF Pulse)

^{1}H t_{90} (μs)	power of ^{1}H channel (db)	$f_C^{(2)}$/% (eq 12b)	$K = \eta_C/\eta_A$ (eq 10b)
4.7	2.5	50	1.98
4.8	2.7	49	2.29
5.1	3	51	2.44
5.2	3.2	50	2.29
5.4	3.4	48	2.15

found difficult to obtain a reliable intensity of the smaller peak (I) against diffusion time. Hence, we simply added the two intensities (I + C) together and treated the system as a "two-phase" system. This may inevitably lead to a systematic error in the derived crystallinity. However, as seen from Figure 7, this systematic error is rather small (<0.5% on an absolute scale) and is discussed more thoroughly in the last section.

Styrene−Isoprene Block Copolymers. From a chemical point of view the isoprene−styrene copolymer (Figure 8) is a rather fascinating polymer due to the irreversibly cross-linking properties of the PI elastomer combined with the easy processing of the thermoplastic PS. The rigid polystyrene domains can form a network of cross-link sites. Moreover, molecular motion within the soft PI domain is of interest due to its prominent influence on the stretching properties of the material. Hence, in a combined SD/^{13}C-CPMAS experiment the signal intensity of the assigned PI peaks will decrease and the signal intensity of the PS peaks will increase with diffusion time.

However, the objective for selecting this particular sample was not motivated by the need to actually determine its phase content but rather that it is an excellent model system to evaluate our method because (a) its phase content is well-known and

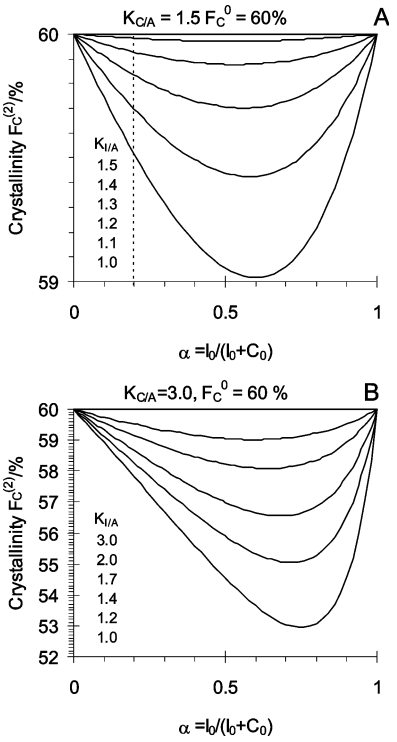

Figure 7. Model calculated "two-phase" crystallinity $f_C^{(2)}$ as a function of the fraction α (= I/(I + C)) of the two crystalline components I and C within the crystalline region of a "three-phase" system (I, C, and A) having a crystallinity of $f_C^0 = 60\%$ and (A) $K_{C/A} = 1.5$ and (B) $K_{C/A} = 3.0$. The solid curves were calculated for different $K_{I/A}$ (component I). The left part of the dotted, vertical line in (A) represents physically realizable α values in this work, indicating that a possible systematic error introduced by our "two-phase" approximation is less than 0.5% (on an absolute scale). Details of the model calculations are presented in the section "Comments Regarding Crystallinity Derived from a "Two-Phase" Model Approximation".

(b) the CP efficiency of PI is rather weak compared to PS. The latter property leads to a highly distorted signal intensity distribution within a CPMAS spectrum and puts particular demands on the quality and potential use of the combined SD/^{13}C-CPMAS method proposed in this work.

The experimental procedure applied to extract the phase content in the PS/PI samples is identical to the one just outlined for the HDPE sample and will therefore not be discussed or commented on any further. We simply replace the symbols A and C in eqs 3−8 by PI and PS, respectively. A contact time $\tau_{cp} = 1$ ms was used, and the actual spin diffusion time was selected within the range of 2−20 ms to ensure no disturbing spin−lattice relaxation effects. A series of SD/^{13}C-CPMAS spectra are shown in Figure 9 (sample S1) for different spin/

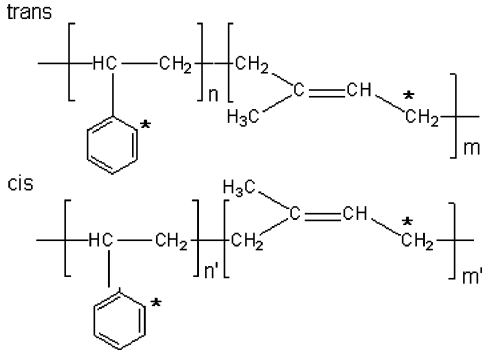

Figure 8. Illustration of the structure of the styrene−isoprene copolymer. The carbons marked with a (*) were chosen to probe the crystalline and the amorphous signals of the copolymer.

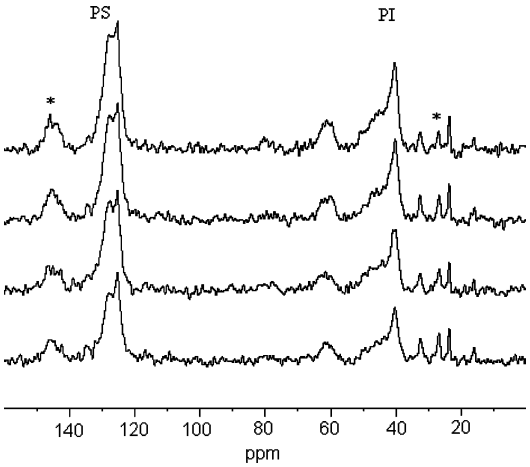

Figure 9. Series of SD/^{13}C-CPMAS spectra of sample S1 for different spin-diffusion times τ_m = 5, 12, 16, and 20 ms.

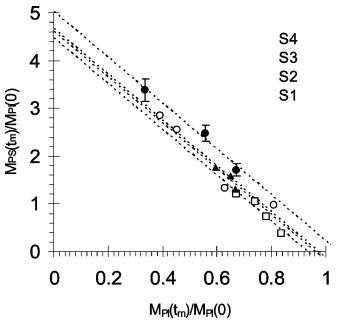

Figure 10. Normalized PS-phase signal intensity $M_{PS}(\tau_m)/M_{PI}(0)$ as a function of the normalized PI-phase signal intensity $M_{PI}(\tau_m)/M_{PI}(0)$ as obtained at different diffusion times τ_m for four different PS−PI block copolymers S1, S2, S3, and S4. The dotted straight lines represent model fits to eq 10b with C and A replaced by PS and PI, respectively. See text for further details.

diffusion times τ_D (= 5, 12, 16, and 20 ms). The actual peaks chosen for this experiment were dictated by the following constraints. To find peaks that have the least overlap with other peaks and, if possible, to find a region which represents both the isomers (cis and trans) of isoprene restricted us to choose the peaks marked by * in Figure 8, which represents the rigid region (PS) and the elastomeric region (PI), respectively. The carbon signal intensity M_{PS}(C)of the PS peak is plotted against the corresponding signal intensity M_{PI}(C) of the PI peak within the PS−PI copolymer (Figure 10). The dotted straight lines represent linear fits to eq 10b with the resulting $K_{PS/PI}$ values summarized in Table 3. Because of the fact that PS and PI are well phase-separated, their phase fractions in terms of proton contents can be easily calculated from their PS weight content. The obtained data are listed in Table 3.

Because of the somewhat limited number of data points in the experiments, the derived standard deviation in $K_{PS/PI}$ ratio is rather high (Table 3). However, by visual inspection of the data (Figure 10) and a statistical evaluation of the individual $K_{PS/PS}$ values, the latter parameters may be assumed to be identical. We therefore fitted all data simultaneously under the constrained that all $K_{PS//PI}$ were identical. The results are shown by the dotted lines in Figure 10 with $K_{PS/PS} = 4.8 \pm 0.4$. All data in Table 3 are derived under this assumption, i.e., the $K_{PS/PS}$ are the same for each sample. From this analysis it follows—within experimental error—that the filter efficiency for all sample are the same and equal to $\epsilon = 1$, i.e., an ideal filter.

Comments Regarding Crystallinity Derived from a "Two-Phase" Model Approximation. For short spin-diffusion time τ_m, we may apply the linear approximation technique to estimate the proton signal intensity M(H;X) as a function of the square root of diffusion time within the three phases X (= A (amorphous), C (crystalline 1), and I (crystalline 2)), i.e.

$$M_I(H;\tau_m) = I_0 R_I \sqrt{t_m}$$

$$M_C(H;\tau_m) = C_0 R_C \sqrt{t_m}$$

$$M_A(H;\tau_m) = A_0 - I_0 R_I \sqrt{t_m} - C_0 R_C \sqrt{t_m} \qquad (14a)$$

where I_0 and C_0 represent the equilibrium (proton) signal intensities of the two "crystalline" regions I and C, and A_0 is the initial signal intensity within the amorphous phase A for $\tau_m = 0$. R_X symbolizes the apparent spin diffusion rate constant within region X. The last equation in 9a is derived under the general constrained that the sum of the proton signal intensities from all the three phases is constant and independent of diffusion time and equal to A_0. It follows that the crystallinity f_C^0 can be written

$$f_C^0 = \frac{I_0 + C_0}{A_0} \qquad (14b)$$

Since it is the carbon nucleus which is detected (after application of a CP pulse sequence), we must transform the proton signals (eq 14a) into the carbon frame. The results are summarized by eq 14c, after dividing eq 14a by A_0 (normalization):

$$Y = \frac{M_{I+C}(C;\tau_m)}{A_0} = \left[\frac{I_0}{A_0} R_I K_{I/A} + \frac{C_0}{A_0} R_C K_{C/A}\right] \sqrt{t_m}$$

$$X = \frac{M_A(C;\tau_m)}{A_0} = 1 - \left[\frac{I_0}{A_0} R_I + \frac{C_0}{A_0} R_C\right] \sqrt{t_m} \qquad (14c)$$

$M_{C+I}(C;\tau_m)$ and $M_A(C;\tau_m)$ represent the carbon signal intensities of the crystalline region (C + I) and the amorphous region (A), respectively. Again, the apparent crystallinity f_C^{app}, as obtained from ^{13}C-CPMAS, can be derived (eq 14b) and reads

$$f_C^{app} = \frac{\eta_I I_0 + \eta_C C_0}{\eta_A (A_0 - I_0 - C_0) + \eta_I I_0 + \eta_C C_0}$$

$$= \frac{I_0 K_{I/A} + C_0 K_{C/A}}{A_0 + I_0 (K_{I/A} - 1) + C_0 (K_{C/A} - 1)} \qquad (14d)$$

Table 3. $K_{PS/PI}$ Ratio, Derived Crystallinity Fraction $f_C^{(2)}$, True Crystallinity Fraction $f_C^{(0)}$, Intercept y_0, and Filter Efficiency ϵ of Samples S1−S4, As Derived by a Combined SD/^{13}CP-MAS Experiment (cf. Figure 1)

sample	$K_{PS/PI} = \eta_{PS}/\eta_{PI}$ (eq 10b)[a]	$f_C^{(2)}$/% (eq 12b)	$f_C^{(0)}$/% (provider)	y_0[b]	ϵ (eq 13b)
S1	5.2 ± 1.5	74 ± 4	72	4.5 ± 0.3	1.07 ± 0.09
S2	5.7 ± 3.5	57 ± 3	58	4.6 ± 0.2	1.04 ± 0.09
S3	4.7 ± 0.6	50 ± 3	54	4.7 ± 0.2	1.03 ± 0.08
S4	4.8 ± 0.8	67 ± 3	68	5.0 ± 0.2	0.96 ± 0.09
$K_{PS/PI,av}$[c]	4.8 ± 0.4				

[a] Defined by the slope of eq 10b (cf. Figure 9) with C and A replaced by PS and PI, respectively. [b] Defined by the intercept of eq 10b with the $M_{PS}(\tau_m)/M_{PI}(0)$ axis (cf. Figure 9). [c] Determined by a simultaneous fit to all curves with $K_{PS/PI}$ assumed to be the same for all samples.

Since the crystalline region is composed of two distinctly different phases (I and C), we introduce the fractional parameter α defined by

$$\alpha = \frac{I_0}{I_0 + C_0} \tag{14e}$$

which simply expresses the fraction of I-phase within the crystalline region (I + C). Inserting this latter equation into eq 14d, we obtain

$$f_C^{app} = \frac{\alpha_0 K_{I/A} + (1-\alpha)K_{C/A}}{1/f_C^0 + \alpha(K_{I/A} - 1) + (1-\alpha)(K_{C/A} - 1)} \tag{14f}$$

From eq 14c we obtain a linear relation between Y and X by eliminating the time variable τ_m. The slope of this line is given by

$$K = \frac{\alpha R_{I/C} K_{I/A} + (1-\alpha)K_{C/A}}{\alpha R_{I/C} + (1-\alpha)} \tag{14g}$$

In this work we have determined the crystallinity of a "three-phase" system (A, I, C) by considering as a "two-phase" system (I + C; A) according to the following strategy: (i) to measure the two crystalline carbon peak intensities (I and C) and the amorphous peak intensity (A) as a function of diffusion time τ_m from a combined SD/^{13}C-CPMAS experiment (eq 14c); (ii) to plot (I + C) against A; (iii) to determine K from the slope of the preceding line (I + C) vs A (eq 14g); (iv) to calculate the f_C^{app} from a simple ^{13}C-CPMAS experiment (eq 14d); (v) replacing $K_{C/A}$ by K in eq 14g and inserting the apparent crystallinity f_C^{app} (eq 14d) into eq 14b to determine the "two-phase" crystallinity, $f_C^{(2)}$.

Since we do not know the apparent spin diffusion rates R_X (eq 14a), we will make the following tentative approximation: $R_X/R_Y = K_X/K_Y$ for any two phases X and Y, which simply states that the spin-diffusion rate is proportional to the enhancement factor; i.e.; "a phase possessing a faster internal molecular motion has a smaller enhancement factor and a correspondingly smaller spin diffusion rate". This assumption leads to the following and final relation between the calculated "two-phase" crystallinity $f_C^{(2)}$ and the actual "three-phase" crystallinity f_C^0:

$$f_C^{(2)} = \frac{1}{1 + (1/f_C^{\,0} - 1)\cdot\dfrac{\alpha K_{I/A}^{\,2} + (1-\alpha)K_{C/A}^{\,2}}{(\alpha K_{I/A} + (1-\alpha)K_{C/A})^2}} \tag{14h}$$

from which the curves in Figure 7 are derived. For a given $K_{C/A}$, it is easily shown that $f_C^{(2)}$ attains its minimum value for the smallest $K_{I/A}$, i.e., for $K_{I/A} = 1$. As can be noted from Figure 7A, the systematic error introduced by the simplification of treating a "three-phase" system as a "two-phase" system is less than 0.5% and, hence, insignificant. However, depending on the actual values of $K_{C/A}$ and $K_{C/I}$, the systematic error may become larger (Figure 7B).

Referring to the experimental data of VanderHart and Khoury,[8] the $K_{C/A}$ ratio of phases C and A seems to be <1.5 for most PE samples, leading to a rather small systematic error by our two-phase approximation. Work is in progress to analyze a three-phase system by the more generalized procedure, represented by eq 11b.

Conclusion

From Table 1 we notice that the apparent crystallinity, as determined from ^{13}C-CPMAS, increases monotonically with increasing contact time and signifies that normal ^{13}C-CPMAS does not yield quantitative information regarding the relative phase content. However, by combining SD and ^{13}C-CPMAS, the derived crystallinity matches that obtained from wide-line ^{1}H NMR for contact times $\tau_{cp} > 1$ ms. For contact times ≤1 ms, the crystallinity becomes slightly smaller by ∼10%. We take this as symptomatic for spatial inhomogeneities, which becomes apparent for short diffusion lengths and thus for short diffusion times. Additional experimental results suggest that the combined SD/CP-MAS technique is reliable under different Hartmann−Hahn conditions. Moreover, a more generalized applicability of the technique is demonstrated by determining the rigid fraction in PS−PI diblock copolymers.

Acknowledgment. E. W. Hansen is obliged to Borealis for financial support in preparing this manuscript during his stay at ECNU in Shanghai, China. This work is also supported by the project of NSFC (No. 20474019) and by Program for Innovative Research Team in University. A special thanks to Prof. Zhongde Xu at East China University of Science and Technology for kindly providing us the PS−PI diblock copolymers.

References and Notes

(1) Stejskal, E. O.; Schaefer, J. J.; Waugh, J. S. *J. Magn. Reson.* **1977**, *28*, 105.
(2) Pines, A.; Gibby, M. G.; Waugh, J. S. *J. Chem. Phys.* **1973**, *59*, 569.
(3) Kolodziejski, W.; Klinowski, J. *Chem. Rev.* **2002**, *102*, 613.
(4) Zhang, S.; Wu, X.; Zhang, H.; Wu, X. *Chem. Phys. Lett.* **1990**, *165*, 465.
(5) Fu, R.; Hu, J.; Cross, T. A. *J. Magn. Reson.* **2004**, *168*, 8.
(6) Hu, W.-G.; Schmidt-Rohr, K. *Polymer* **2000**, *41*, 2979.
(7) Hou, G.; Deng, F.; Ye, C.; Ding, S. *J. Chem. Phys.* **2006**, 124.
(8) VanderHart, D. L.; Khoury, F. *Polymer* **1984**, *25*, 1589.
(9) Hartmann, S. R.; Hahn, E. L. *Phys. Rev.* **1962**, *128*, 2042.
(10) Schaefer, J. J.; Stejskal, E. O. *J. Am. Chem. Soc.* **1976**, *98*, 1031.
(11) Mehring, M. *Principles of High Resolution NMR in Solids*; Springer-Verlag: New York, 1983.
(12) Zhang, L.; Chen, Q.; Hansen, E. W. *Macromol. Chem. Phys.* **2005**, *206*, 246.
(13) Voigt, G.; Kimmich, R. *Polymer* **1980**, *21*, 1001.
(14) Hansen, E. W.; Kristiansen, P. E.; Pedersen, B. *J. Phys. Chem. B* **1998**, *102*, 5444.

(15) Litvinov, V. M.; Penning, P. *Macromol. Chem. Phys.* **2004**, *205*, 1721.E.
(16) Hedesiu, C.; Demco, D. E.; Kleppinger, R.; Buda, A. A.; Blümich, B.; Remerie, K.; Litvinov, V. M. *Polymer* **2007**, *48*, 763.
(17) Uehara, H.; Aoike, T.; Yamanoble, T.; Komoto, T. *Macromolecules* **2002**, *35*, 2640.
(18) Kitamaru, R.; Horii, F.; Murayama, K. *Macromolecules* **1986**, *19*, 636.
(19) Kimura, T.; Neki, K.; Tamura, N.; Horri, F.; Nakagawa, M.; Odani, H. *Polymer* **1992**, *25*, 4114.
(20) Kuwabara, K.; Kaji, H.; Horii, F.; Bassett, D. C.; R. H. Olley, R. H. *Macromolecules* **1997**, *30*, 7516.
(21) Kuwabara, K.; Horii, F. *Macromolecules* **1999**, *32*, 5600.

MA0707786